Final Technical Report
U.S. Geological Survey
National Earthquake Hazards Reduction Program
USGS External Award # G16AP00060
Start Date: March 1, 2016
End Date: June 30th, 2018

Pilot Paleoseismic Investigation of Faults in the North Valleys, Reno, NV

Seth Dee, Alan R. Ramelli, and Richard D. Koehler
Nevada Bureau of Mines and Geology
1664 N Virginia St.
University of Nevada Reno / MS178
Reno, Nevada 89557-0178
Office 775-784-6691
Fax 775-784-1709
sdee@unr.edu
ramelli@unr.edu
rkoehler@unr.edu

http://www.nbmg.unr.edu/

Additional project support provided by UNR PhD student Conni De Masi

ABSTRACT

A series of fault-bounded basins located just north of Reno, Nevada, collectively known as the North Valleys, form an important structural linkage between some of the most active faults in the Basin and Range province: the Carson Range fault system to the south; and northwest-striking dextral faults of the northern Walker Lane to the north (e.g. Honey Lake and Warm Springs Valley faults). The southern edge of the North Valleys is within 5 km of downtown Reno and the area is undergoing rapid development. Despite their tectonic significance and location, faults in the North Valleys have received relatively little paleoseismic attention to date. To better characterize the seismic hazard posed by the faults this study used recently acquired lidar data to remap faults in Lemmon and Antelope Valleys and paleoseismic trenching to determine the earthquake history and slip-rate of the Freds Mountain fault. This effort is a pilot investigation intended to help guide future research on the paleoseismic history and seismic hazard in the area.

Two trenches were excavated as parts of this study. The first trench crosses a prominent scarp on a mapped, unnamed fault at the base of the Granite Hills along the western edge of Lemmon Valley. The trench exposed a package of lacustrine sediments and no evidence for faulting. It was determined that the scarp is a wave cut shoreline formed by a Pleistocene lake in Lemmon Valley. Identification of the fault as a shoreline facilitated a revaluation of the Pleistocene lake history in Lemmon Valley, new fault mapping, and new slip-rate estimates.

A second trench was excavated across a scarp on the Freds Mountain fault (FMF) in Antelope Valley. The trench exposed faulted alluvial-fan deposits, evidence for four surface rupturing earthquakes, and yielded a new vertical displacement estimate. Age estimates of the paleo-earthquakes and displaced stratigraphy are pending results of Optically Stimulated Luminescence (OSL) and bulk radiocarbon sample analysis. A new lidar-based fault and geologic map of the FMF was produced delineating two fault segments and the relative ages of faulted alluvial-fan deposits.

INTRODUCTION

The North Valleys are a series of north- to north-northeast trending, fault-bounded alluvial basins separated by bedrock ranges (Figures 1 and 2) located north of Reno, NV, and straddling the Nevada-California state line. Principal named Quaternary faults in the North Valleys include the Last Chance fault zone, Petersen Mountain fault, Freds Mountain fault, and Spanish Springs Valley fault (Figures 1 and 2). Other mapped Quaternary faults include discontinuous fault traces in Cold Springs, and Lemmon Valleys (Figure 2). The Reno metropolitan area has expanded into the North Valleys in recent years and earthquakes along these faults pose surface fault rupture and ground shaking hazards to local residents and infrastructure. The 2018 Working Group on Nevada Seismic Hazards identified faults on the North Valleys as a priority for further study to better characterize fault parameters (Koehler and Anderson, in press).

The 2014 update of the National Seismic Hazard Map (NSHM) includes the Petersen Mountain, Spanish Springs Valley and Freds Mountain faults as seismic sources (Peterson et al., 2014). The geologic slip-rates assigned to each of these three NSHM sources are largely nominal values ranging from 0.065 mm/yr to 0.131 mm/yr based on little or no fault-specific geologic data. The Last Chance fault, located in California, is included in the Uniform California Earthquake Rupture Forecast, Version 3 (UCERF3) model (Field et al., 2013). UCERF3 assigned a geologic slip-rate of 0.01 mm/yr to the Last Chance fault and recommended it for re-evaluation as part of UCERF4.

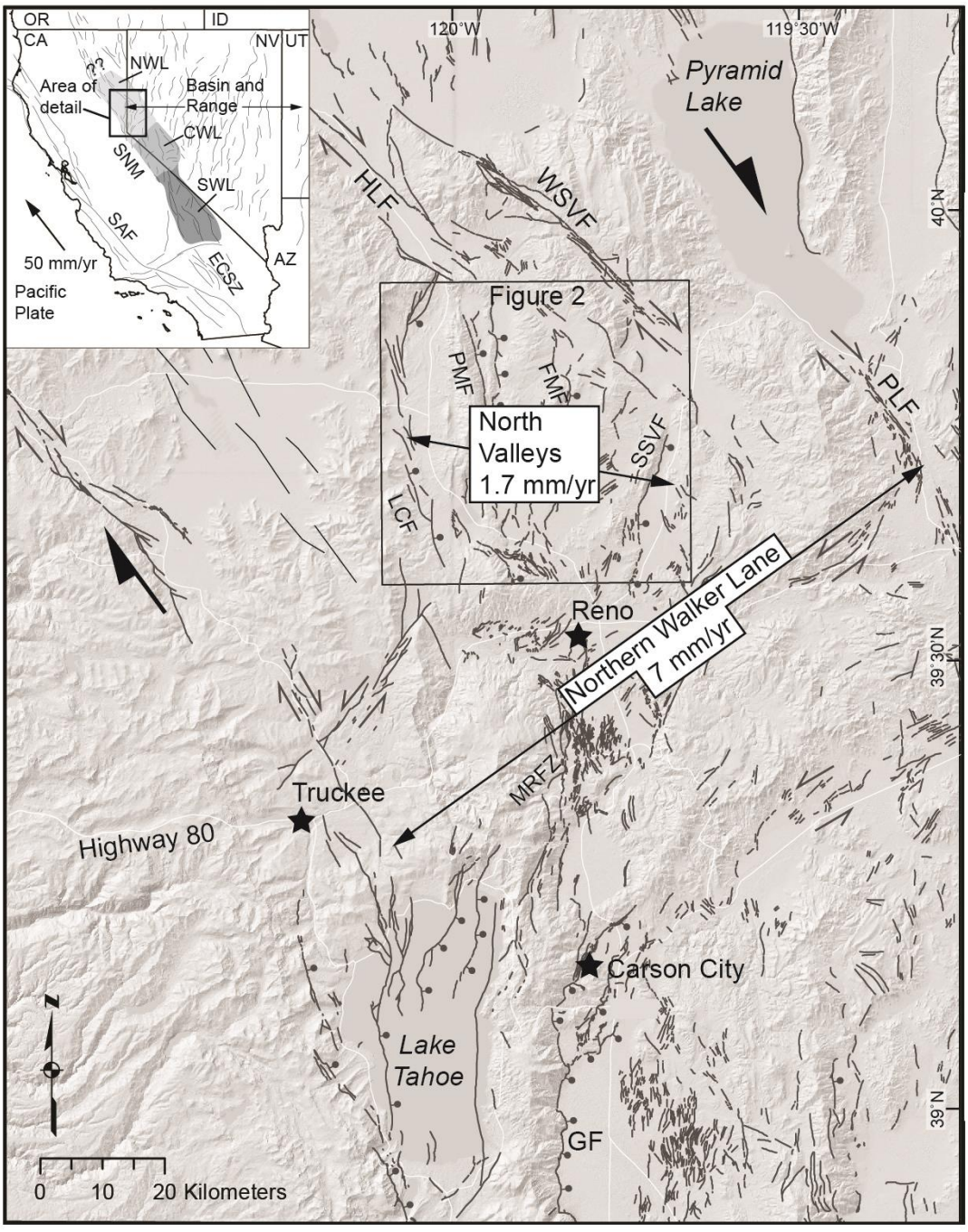

Figure 1 Regional map of Quaternary faults (U.S. Geological Survey, 2006) showing the location of the North Valleys area with respect to the northern Walker Lane and the Basin and Range Province. Geodetically determined rates of extension across the entire North Valleys and across the northern Walker Lane are shown in white boxes with arrows (Borman, 2013). Location of Fig. 2 shown by black box. Insetmap shows location of the North Valleys with respect to the regional tectonic setting. The Walker Lane belt is shown as a shaded belt including the southern Walker Lane (SWL, dark gray), central Walker Lane (CWL, medium gray), and northern Walker Lane (NWL, light gray). SAF, San Andreas fault; SNM, Sierra Nevada microplate; ECSZ, eastern California shear zone; HLF, Honey Lake fault; WSVF, Warm Springs Valley fault; PLF, Pyramid Lake fault; SSVF, Spanish Springs Valley fault; FMF, Fred's Mountain fault; PMF, Peterson Mountain fault; MRFZ, Mount Rose fault zone GF, Genoa fault.

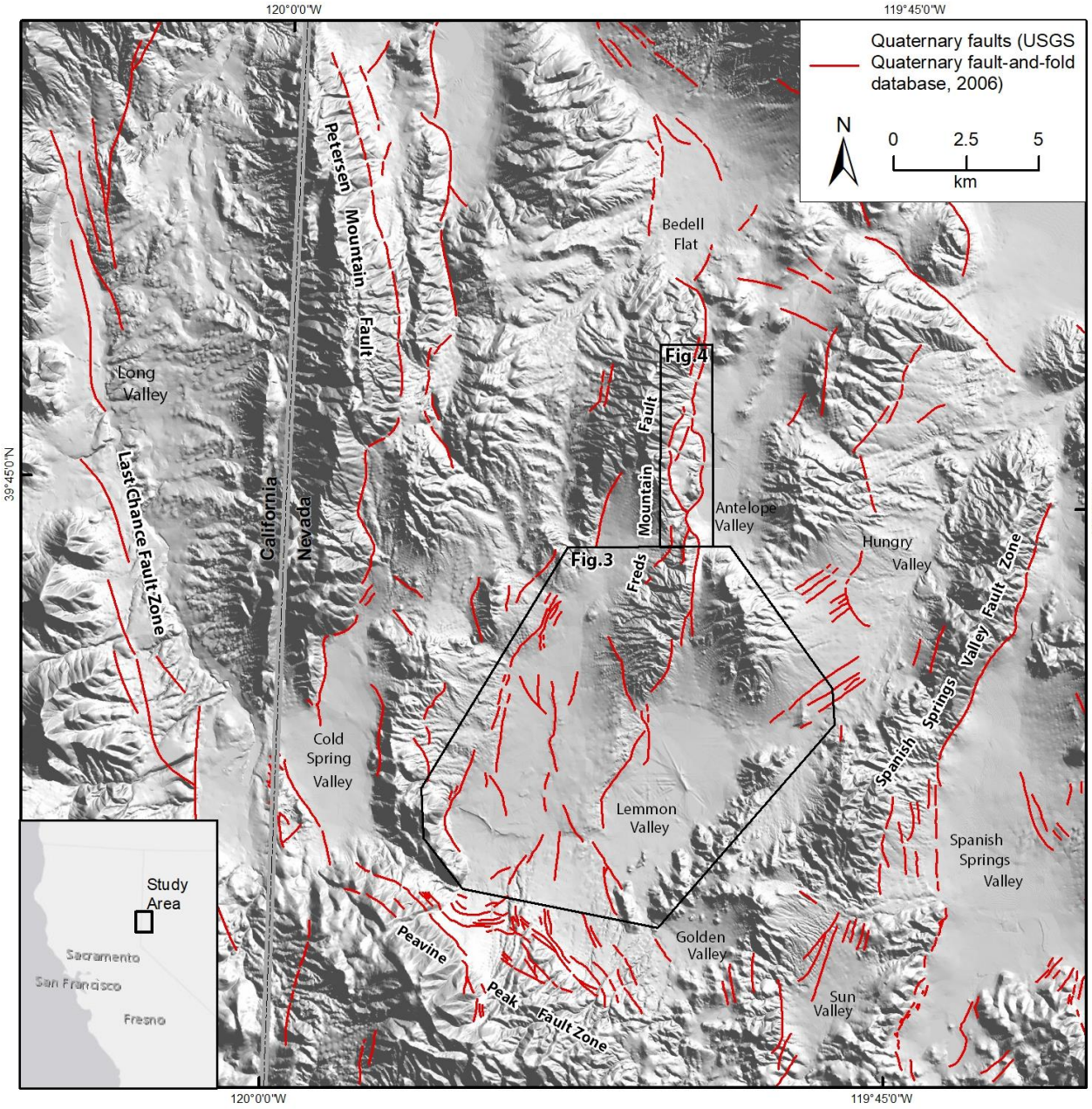

Figure 2 - Quaternary faults (U.S. Geological Survey, 2006) in the North Valleys study area.

The goals of this study include using newly available lidar data to re-map several of the faults in the North Valleys and to determine the earthquake history and slip-rate of one of the faults through paleoseismic trenching. This effort is a pilot investigation that will help guide future research on the paleoseismic history and seismic hazard in the area.

GEOLOGIC AND TECTONIC SETTING

The North Valleys are bounded by east-dipping normal faults and situated directly south of the dextral Honey Lake and Warm Springs Valley fault zones of the northern Walker Lane (Wesnousky, 2005) (Figure 1). To the south, the North Valleys faults are truncated by the Peavine Peak fault, a prominent northwest-striking range front fault that is interpreted as having normal oblique (dextral) slip and to be the likely northern continuation of the Carson Range fault system (CRFS) (Ramelli et al., 2003; 2005; Figure 1). The North Valleys normal faults accommodate extension and associated crustal thinning near the southeastern termination of the dextral Honey Lake and Warm Springs Valley fault zones (Faulds et al., 2005), and form a trailing extensional imbricate fan (e.g., Woodcock and Fisher, 1986). This diffuse zone of extension coalesces southward and merges with faults of the CRFS including the Mount Rose fault zone and the Genoa fault (Figure 1; Faulds et al., 2005). Therefore, the North Valleys faults serve as an important tectonic linkage between the Honey Lake and Warm Springs Valley fault zones and the CRFS, and likely accommodate a significant portion of the relatively high tectonic strain found on those structures.

Geodetic studies estimate ~7 mm/yr of dextral shear strain across the Northern Walker Lane accommodated largely by the left-stepping en echelon Pyramid Lake, Honey Lake and Warm Springs Valley fault zones (Hammond and Thatcher, 2007; Hammond et al., 2011; Figure 1). A late Quaternary geologic slip-rate of 1.8 – 2.4 mm/yr was estimated for the Warm Springs Valley fault zone through mapping and Terrestrial Cosmogenic Nuclide (TCN) dating of an offset alluvial-fan (Gold et al., 2013). Trenching of the Warm Springs Valley fault revealed evidence for eight surface-rupturing earthquakes since 21±4 ka (dePolo and Ramelli, 2004; dePolo, 2006). Holocene slip-rate estimates of the Honey Lake fault zone range from ~1-2 mm/yr (Wills and Borchardt, 1993, Turner et al., 2008; Gold et al. 2017). Trenching of the fault (Turner et al., 2008) revealed four surface-rupturing earthquakes since 7.0 ka.

Trenching of the Peavine Peak fault exposed evidence for four or five surface-rupturing events over the past 6000-7000 years (Ramelli et al., 2003; 2005). Clast alignments within the fault zone suggest approximately equal components of normal and right-lateral offset, indicating a Holocene slip-rate on the order of 1 mm/yr. The 6000-7000 year time range was based on six bulk radiocarbon samples, with the older ages interpreted as most representative of the age of faulted fan deposits. Bulk samples can have large uncertainties, so one sample from the fan deposits was reanalyzed and yielded an age of 3195 +/- 15 ypb (3440-3380 cal B.P.) (Puseman, 2010). These findings indicate that Holocene earthquake recurrence on the Peavine Peak fault is comparable to the CRFS to the south.

Trenching of the Genoa fault (southern CRFS; Figure 1) exposed two large-displacement events during the late Holocene and yielded an estimated slip-rate of 2-3 mm/yr (Ramelli et al., 1999). Subsequent work, including refined radiocarbon dating, indicated that the two events occurred about 300-400 cal B.P. and 1700-1800 cal B.P., and also showed that the northern part of the CRFS ruptured at similar times (Rood, 2011; Ramelli and Bell, 2014). Geodetic estimates of slip on the Genoa fault are much lower at 0.3 mm/yr to 0.4 mm/yr (Hammond et al., 2011). Given the recency of the last earthquake on the Genoa fault, one

possible explanation for the discrepancy is temporal variation in strain accumulation early in the faults recurrence cycle.

Very little paleoseismic characterization has been done on faults in the North Valleys. The faults were mapped in detail by Bell (1984) using low sun angle aerial photos, and as part of various geologic quadrangle and compilation maps (Soeller and Nielsen, 1980; Cordy, 1985; Garside, 1993; Garside et al. 2010; Ramelli et al., 2012). Geodetic studies by Borman (2013) estimate that north-striking faults of the North Valleys collectively accommodate up to 1.7 mm/y of extension and 0.3 mm/y of dextral slip. Koehler (2018) performed a reconnaissance level assessment of the tectonic geomorphic expression of the faults determining that they are capable tectonic structures and calculated slip-rates on the Freds Mountain, Petersen Mountain and Spanish Springs Valley faults using scarp profile and relative age estimates of displaced surfaces.

This report is divided into two sections below. The first section is focused on the results of trenching, fault mapping and a re-examination of the pluvial lake history in Lemmon Valley. The second section presents results of paleoseismic trenching and fault mapping on the Freds Mountain Fault in Antelope Valley.

LEMMON VALLEY

Lemmon Valley is actually two hydrographic sub-basins bisected by an uplifted plateau of Tertiary sediments forming a relatively low drainage divide (Figure 3). Both sub-basins are occupied by playa lakes that are historically dry for much of the year, but have been at record levels since 2016. The surrounding highlands are comprised of largely granitic rocks overlain by Tertiary andesitic volcanic rocks (Cordy, 1985 and Soeller and Niellson, 1980). Tertiary alluvial and fluvial-lacustrine sediments unconformably overly the bedrock throughout the basin lowlands. Quaternary sediments in the basins include deposits from late-Pleistocene Lake Lemmon, including sandy beach bar and lacustrine silt deposits. (Soeller, 1978; Cordy, 1985).

Previously mapped faults in the western sub-basin are included in the USGS Quaternary fault database as “unnamed faults in Lemmon Valley” (USGS, 2006). The faults include a range-front fault along the eastern edge of the Granite Hills, intrabasin faults in the vicinity of Silver Lake, west-facing scarps near Stead Airport, and a collection of scarps converging northward towards the southwestern extent of Fred’s Mountain (Szecsody, 1983; Nitchman and Ramelli; 1991). Koehler (2018) referred to this collection of faults as the Western Lemmon Valley fault zone (WLVFZ) and that name will be used in this report.

The eastern Lemmon Valley sub-basin is bound on the west by the southernmost section of the Fred’s Mountain Fault (FMF) (Figure 3). The FMF is an east dipping, down to the east normal fault. To the north in Antelope Valley the fault runs along the eastern front of Fred’s Mountain and is the focus of the next section in this report (Figure 3). In Lemmon Valley the fault has previously been as a piedmont scarp along the eastern side of an unnamed mountain whichcontinues southward through the middle of Lemmon Valley (USGS, 2006). Cordy (1987) excavated two trenches across a scarp on a mapped intrabasin section of the fault in northern Lemmon Valley. Both trenches exposed near vertical fractures and infilled fissures, interpreted as resulting from the most recent surface ruptures. Correlation of a sand lens exposed in the trench, on either side of the scarp, was used to infer a history of displacement, however no shear zone was documented. Koehler (2018) used lidar data to profile scarps on the Lemmon Valley segment of the FMF and inferred vertical slip-rates of 0.01-0.3 mm/yr.

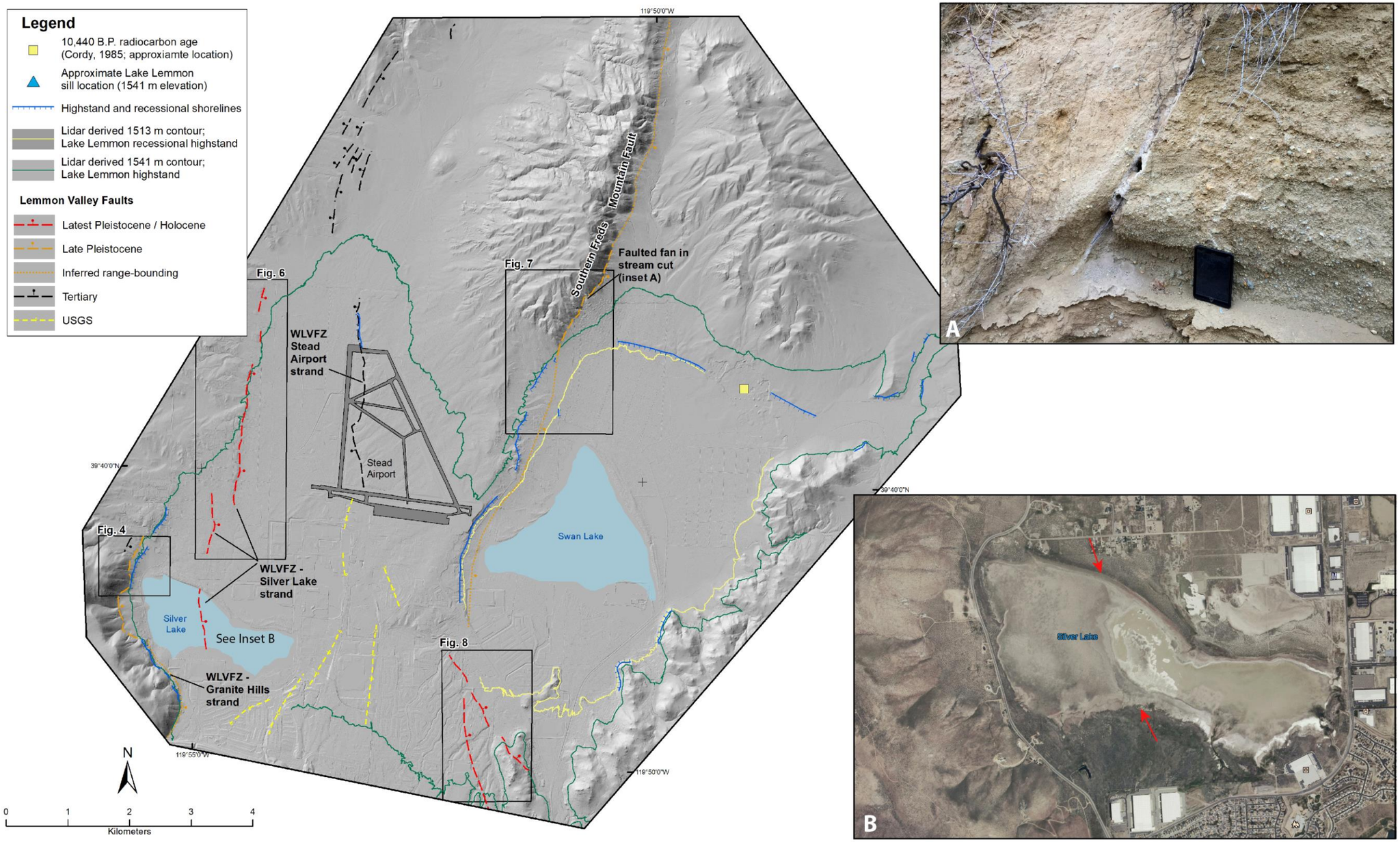

Figure 3 - Faults, shorelines and extent of late Pleistocene Lake Lemmon in Lemmon Valley. Inset photo A shows faulted fan deposits exposed in a stream cut along the trace of the southernmost Freds Mountain Fault (location of photo marked on map). Inset B shows Google Earth satellite imagery of Silver Lake from 2011 during low water levels. An east facing scarp in the lake is interpreted from the imagery, the scarp is on strike with other WLVFZ Silver Lake strand scarps.

Granite Hills Trenching

In October of 2016 a paleoseismic trench was opened using a track mounted excavator across a prominent scarp on the mapped trace (Szecsody, 1983; USGS, 2006) of the WLFFZ near the eastern range front of the Granite Hills (Figures 3 and 4). This fault trace was chosen for trenching due to its proximity to a growing population center and to investigate possible linkage between the earthquake history of the WLVFZ and the Peavine Peak fault to the south. The site was chosen because the 5.5 m high scarp in an alluvial-fan surface appeared likely to yield evidence of repeated late-Quaternary earthquakes.

The 22 m long trench was excavated to a maximum depth of 3.5 m (Figures 4 and 5). No evidence for faulting was identified in the trench exposure (Figure 5). The lower beds in the trench (Units L10 to L1 on Figure 5) are moderately to well sorted, thinly bedded, pebbly sand, interbedded with massive beds of sandy silt. Pebbly sand beds have wave ripples and Tiger beetle burrows indicative of shallow water deposition and periodic subaerial exposure adjacent to a pluvial lake (Reheis et al., 2014). These deposits are interpreted to be lacustrine, with wave-sorted clastic material sourced from local highlands interbedded with fine sediment deposited by sub-aqueous debris flows or storm deposits. The lacustrine sediments are overlain by massive, poorly sorted, silty sands with gravels interpreted as interbedded alluvial-fan and eolian deposits (Unit AF1 on Figure 5). A 30-60 cm thick Bt soil horizon with blocky pedogenic structure drapes the scarp topography (Figure 5). Several vertical fractures with no discernible displacement extend through the trench stratigraphy, but do not continue into the capping soil. The lack of faulted stratigraphy and the abundant lacustrine sediments in the trench indicate that the scarp is a shoreline eroded by waves on the west end of late-Pleistocene Lake Lemmon.

Late Pleistocene Lake Lemmon

Late Pleistocene Lake Lemmon was first named by Hubbs and Miller (1948), and described in greater detail by Soeller (1978). Lacustrine deposits were subsequently depicted on the Reno NW (Soeller and Niellson, 1980) and Reno NE (Cordy, 1987) geologic quadrangle maps of Lemmon Valley. These mapped deposits indicated that the lake reached an elevation of 1519 m, well below the 1541 m sill elevation at the lowest outlet of the basin.

The trench stratigraphy (Figure 5) and new lidar based shoreline mapping (Figure 3) indicate that Lake Lemmon likely overtopped the 1541 m sill elevation. The highest elevation lacustrine sediments identified in the Granite Hills trench have an elevation of 1533 m, adjacent shoreline angles range in elevation from 1534-1536 m, and the top of the shoreline varies between 1538 and 1541 m. A lidar derived elevation contour at 1541 m, shown in Figure 3, allowed for identification of additional shoreline remnants of the Lake Lemmon highstand. Spillover at the sill would have resulted in late Pleistocene hydrologic connection, via Hungry Valley, between Lake Lemmon and the topographically much lower Lake Lahontan to the east. The age of the Lake Lemmon highstand is unknown but it is reasonable that lake may have reached its maximum elevation synchronously with the late-Pleistocene Seehoo highstand of Lake Lahontan at 13,000 ^{14}C B.P (~15,300 cal. B.P.) (Adams and Wesnousky, 1999; Adams et al., 2008). The lacustrine deposits in the trench (L1-L10) are beneath alluvial-fan deposits (AF1), and the shoreline is eroded into that fan surface. This relationship suggests that the fan is older than the lake highstand and the underlying lacustrine sediments may be part of a pre- late Pleistocene lake.

A recessional highstand of Lake Lemmon is recorded by a prominent set of beach bars in eastern Lemmon Valley with shoreline angles at 1515 m in elevation (contour shown on Figure 3). Cordy (1985) reported a ^{14}C age of 10,440 B.P. from a mammoth bone in this deposit (approximate location shown on Figure 3).

Lidar derived contours at the shorelines associated with the 1541 m highstand and the 1515 m recessional shoreline facilitated a revaluation of fault mapping in the valley, discussed below.

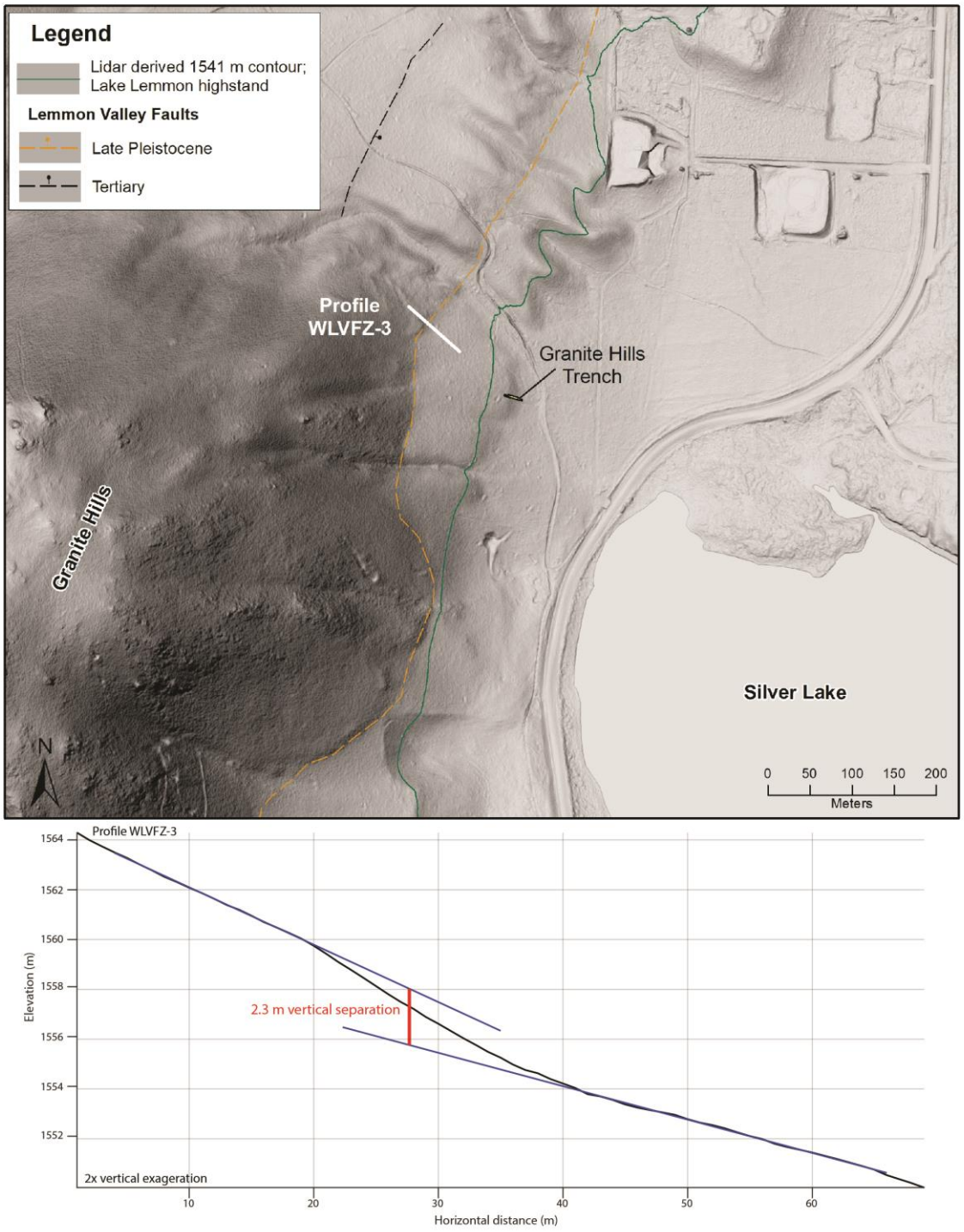

Figure 4 - Lidar slopeshade map of the fault at the foot of the Granite Hills and the location of the Granite Hills trench (figure location shown on Figure 3). Trench log shown in Figure 5. The trench crossed a 5.5 m scarp now recognized to be a shoreline from the highstand of late Pleistocene Lake Lemmon which reached approximately 1541 m in elevation (contour shown in green). Profile across a fault scarp along the Granite Hills strand of the WLVFZ. Scarp displaces inferred late-Pleistocene fan

Granite Hills Trench Log

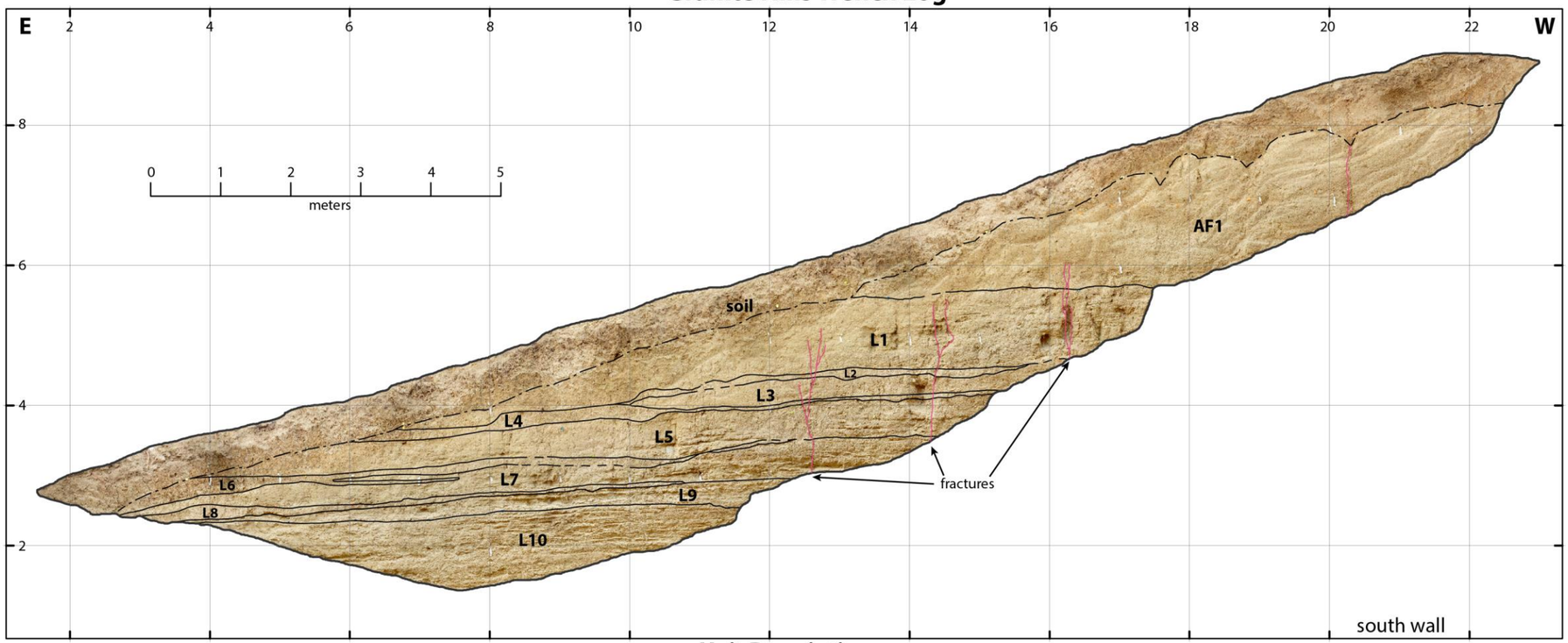

Unit Descriptions

Soil – dry color: yellowish brown 10yr 5/6, sandy clay with pebbles, 10% clasts, 10 cm max clast, blocky pedogenic structure, soil is 30-60cm thick and overprints original stratigraphy.

AF1 - dry color: pale brown 10yr 6/3, silty sand with gravels, 10% clasts, 10 cm max clast, angular to subangular, granitic, medium dense, poorly sorted, massive with gravel rich interbeds up to 10 cm, sharp planar lower contact. **Alluvial fan with eolian sand**

L1- dry color: pale brown 10yr 6/3, pebbly sand, 5% clasts, 2 cm max clast generally less than .5 cm, angular to subangular, granitic, medium dense, moderately well sorted, bedding thin to 10 cm, common sandy silt interbeds up to 10cm, sandy silt beds makeup approx 30% of unit, minor cross bedding in sandy beds, sharp to gradational and planar lower contact, **lacustrine pebbly sand**

L2 – dry color: light brownish gray 10yr 6/2, sandy pebbly silt (fine pebbles, ganitic) , very stiff, massive, poorly sorted, lower contact gradational and undulatory. **Possible storm or debris flow pulse of fine sediment**

L3 – dry color: pale brown 10yr 6/3, pebbly sand, 15- 20% clasts, 5 cm max clast generally less than 2 cm, angular to subangular, granitic, medium dense, moderately well sorted, bedding thin to 10 cm, common silt interbeds up to 10 cm, locally unit is very silty, minor cross bedding, sharp and planar lower contact, **lacustrine pebbly sand**

L4- wet – dry color: brown 10yr 5/3, sandy silt (fine sand), <2% fine pebbles, medium stiff, massive, poorly sorted, lower contact gradational and undulatory, variable thickness. **Possible storm or debris flow pulse of fine sediment**

L5- dry color: light brownish gray (10yr 6/2) pebbly sand, 15- 30% clasts, 3cm max clast with one 15 cm cobble, generally less than 1 cm, angular to subangular, granitic clasts, loose to medium dense, moderately to well sorted, thin bedding, max bed thickness 20 cm, common silt interbeds up to 20cm, minor cross bedding, sharp and broadly undulating lower contact, **lacustrine pebbly sand**

L6 – dry color: brown 10yr 5/3, sandy silt (fine sand),<5% fine pebbles, medium stiff, massive, poorly sorted, lower contact gradational. **Possible storm or debris flow pulse of fine sediment**

L7 - dry color: light brownish gray (10yr 6/2), pebbly sand, 15- 20% clasts, 2cm max clasts, generally less than 1 cm, angular to subangular, granitic clasts, loose, moderately to well sorted, thinly (laminar) bedded, max bed thickness 2 cm, very thin to 2 cm thick silt interbeds, particularly near top of unit. minor cross bedding and wave ripples, sharp and planar lower contact. **lacustrine pebbly sand**

L8 – dry color: brown 10yr 5/3, sandy silt (fine sand),<5% fine pebbles, medium stiff, massive, poorly sorted, lower contact sharp, planar to wavy. **Possible storm or debris flow pulse of fine sediment**

L9 – dry color: light brownish gray (10yr 6/2), pebbly sand, 10-20% clasts, 2 cm max clasts, generally less than 0.5 cm, angular to subangular, granitic, loose, moderately to well sorted, thinly (laminar) bedded, max bed thickness 0.5 cm, very thin beds with concentrated heavy minerals, common fossil beetle? burrows, minor cross bedding, sharp and planar lower contact. **lacustrine pebbly sand**

L10 – dry color: light brownish gray (10yr 6/2), pebbly sand, with fine grained interbeds (silt>clay), 20% clasts with some clast supported pebble rich interbeds, clasts up to 5 cm diameter, generally less than 1 cm, angular to subangular, granitic, loose, moderately to well sorted, thinly bedded, max bed thickness 5cm, loose, flat bedding, locally cross bedded, some wave ripples, few fossil beetle? burrows. **lacustrine pebbly sand**

Figure 5 – Log of the Granite Hills trench south wall. Log shows flat lying lacustrine stratigraphy (units L1 to L10) overlain by alluvial-fan deposits mixed with eolian sand. Several fractures cut the stratigraphy but no faulting was observed.

New Fault Mapping in Lemmon Valley

A new fault map of Lemmon Valley is shown on Figure 3. The mapping utilized new lidar data and field mapping to document fault scarps, fault exposures, and shorelines in undeveloped parts of the valley. The improved understanding of the extent and elevation of late Pleistocene Lake Lemmon supported a revaluation of several previously mapped scarps that are now interpreted to be shorelines. Faults in Lemmon Valley are divided into five classes on Figure 3:

Latest Pleistocene / Holocene faults (red) – Scarps in alluvial-fan and lacustrine deposits that are located within the extent of Lake Lemmon (below the 1541 highstand), and along strike scarps that extend beyond the lake boundaries. The preservation of these scarps within the lake basin suggests that they may post-date the lake highstand, and displace latest Pleistocene lacustrine stratigraphy.

Late Pleistocene faults (orange) – Scarps in late Pleistocene surfaces (including along strike continuations into older sediments) and/or range-bounding faults where late Pleistocene fan deposits have been observed to be in fault contact with bedrock.

Inferred range-bounding faults (orange dotted) – Range-bounding faults inferred to bound uplifted highlands and bedrock ranges but lacking observed fault scarps or exposure in Quaternary sediments. Includes likely buried faults with surface expression modified by shoreline erosion.

Tertiary (black) – Fault scarps entirely within Tertiary deposits. Many of these scarps have sharp morphology in poorly lithified sediments indicating that a pre-Quaternary age of formation is unlikely, however the lack of offset in Quaternary surfaces precludes an age estimate.

USGS (yellow) – Faults included in the USGS Quaternary fault database that are located in areas modified by urban development. Reevaluation of the faults using lidar and current imagery was not feasible.

Western Lemmon Valley Fault Zone (WLVFZ)

The WLVFZ consists of three main strands, the Granite Hills strand, the Silver Lake strand, and the Stead airport strand. The Silver Lake strand (Figure 3) is comprised of a semi-continuous collection of east facing scarps in late Pleistocene fan deposits and possibly in latest Pleistocene or younger lacustrine deposits (Figure 6). The scarps are located partially within the extent of the Lake Lemmon highstand and continue north into alluvial-fan deposits that are above the 1541 m shoreline elevation. The southernmost mapped trace of the segment is located beneath Silver Lake along a scarp visible in satellite imagery collected during low lake levels (Figure 3, inset B). The presence of prominent scarps within the boundaries of Lake Lemmon suggests that they could displace latest Pleistocene lacustrine sediments. In northern Lemmon Valley a cluster of east and west facing scarps in Tertiary sediments are on strike with the young scarps to the south (Figure 3), suggesting similar origins, but do not displace Quaternary deposits.

The Granite Hills strand of the WLVFZ is characterized by east-facing fault scarps in alluvial-fan deposits along the east side of Granite Hills, west of, and topographically above, the Lake Lemmon shoreline and the Granite Hills trench site (Figures 3 and 4). The shoreline is eroded into the faulted fan deposits and therefore the deposits likely predate the age of the highstand. These scarps continue northward displacing a pediment surface in Tertiary sediments.

The Stead Airport strand is defined by a west-facing scarp situated just west of the airport (Figure 3). The scarp is up to 6 meters high in Tertiary sediments and is likely antithetic to the principal east-dipping,

graben-bounding structures to the west. The scarp is buried to the north by latest Pleistocene to Holocene alluvial-fan deposits indicating no recent displacement.

Three scarp profiles (Figures 4 and 6) were measured on late Pleistocene or younger scarps using lidar DEMs, and vertical separation values were calculated using the *Scarp Offset* script developed by Chris DuRoss at the USGS. The vertical separation values were converted to slip rates assuming inferred ages for the faulted deposits (Table 1). Profiles WLVFZ-1 and WLVFZ-2 cross the Silver Lake strand and have vertical separations of 5.6 m and 6.7 m, respectively (Figure 6). The offset deposits are inferred to be late-Pleistocene in age (12-120 ka), yielding vertical slip-rates of 0.05-0.6 mm/yr. Profile WLVFZ-1 is located within the lake highstand and may displace latest Pleistocene Lake Lemmon lacustrine deposits, a scenario that favors the higher slip-rate estimates. Profile WLVFZ-3 crosses the Granit Hills strand where the fault displaces alluvial-fan deposits with an inferred late Pleistocene age (Figure 4). Vertical separation across the fault is 2.3 m yielding a vertical slip-rate of 0.02-0.2 mm/yr. The Granite Hills strand, and profile WLVFZ-3, individually only captures a portion of the total displacement across the fault zone. The combined vertical displacement across the Granite Hills and Silver Lake strands approaches 9 m suggesting that the vertical deformation rate across the zone may be better estimated at 0.075-0.75 mm/yr. However, this rate does not include potential antithetic contributions from the Stead Airport strand.

Southernmost Freds Mountain Fault (eastern Lemmon Valley)

The main trace of the Freds Mountain fault (FMF) traverses a topographic divide south of Antelope Valley and continues southward into Lemmon Valley (Figure 3). The FMF in Antelope Valley is discussed in the next section of this report. The northernmost section of the FMF in Lemmon Valley has no discernable scarps in Quaternary sediments and bounds a weakly faceted range front (Figure 3). To the south the range front becomes increasingly faceted and a newly identified stream cut exposes Pleistocene sediments faulted against bedrock (inset A on Figure 3 with location marked on Figure 7). South of where the range front ends the fault continues as a small scarp in late Pleistocene alluvial-fan deposits. Profile FMF-1 across the scarp has a measured vertical separation of 0.9 m (Figure 7). This scarps ends near the 1541 m lake highstand elevation at a small shoreline, suggesting that faulting predates the lake highstand, and any scarps that continue into the lake basin have been smoothed by lacustrine deposition or erosion. The scarp that was trenched by Cordy (1987) is on strike with the scarps mapped to the north (Figure 7). However, the base of that scarp has a uniform elevation at approximately 1511 m, close to the elevation of the recessional highstand shoreline (1513 m). This observation, in conjunction with the lack of evidence for surface rupture in the trenches by Cordy, suggests that this is not the active fault trace. Instead the fault likely continues as a concealed trace to the south-southwest along the base of a prominent escarpment between the Stead airport and Swan Lake (Figure 3). Uplifted Tertiary sediments exposed in the escarpment supports the presence of a concealed fault. This escarpment would have been heavily modified by the Lake Lemmon highstand and pre-existing late-Pleistocene fault scarps may have been eroded or buried by lake processes.

South of Swan Lake are two north-northwest trending fault scarps in alluvial-fan surfaces (Figures 3 and 8). To the south these same fan surfaces are mapped by Ramelli et al. (2011) as being middle to late Pleistocene in age, though a late Pleistocene age is preferred. The scarps are primarily below the elevation of the Lake Lemmon highstand and may post date the lake highstand, though there is no clear evidence that latest Pleistocene lacustrine sediments are displaced. Urban development is extensive on the scarps but a single profile (FMF-2) yielded a vertical separation measurement of 2.8 m (Figure 8). Using the Ramelli et al. (2012) age for the fan surface the vertical slip-rate is <0.01-0.2 mm/yr. If the scarps post-date the lake highstand then the slip-rate may be closer to the higher estimate. The lack of continuity between these, possibly young, scarps in the south and the inferred / buried southern FMF to the north

suggest that the two structures may have different paleoseismic histories. Based on their generally northwestern orientation, these faults may represent eastern strands of the similarly oriented Peavine Peak fault zone rather than part of the Fred's Mountain fault zone.

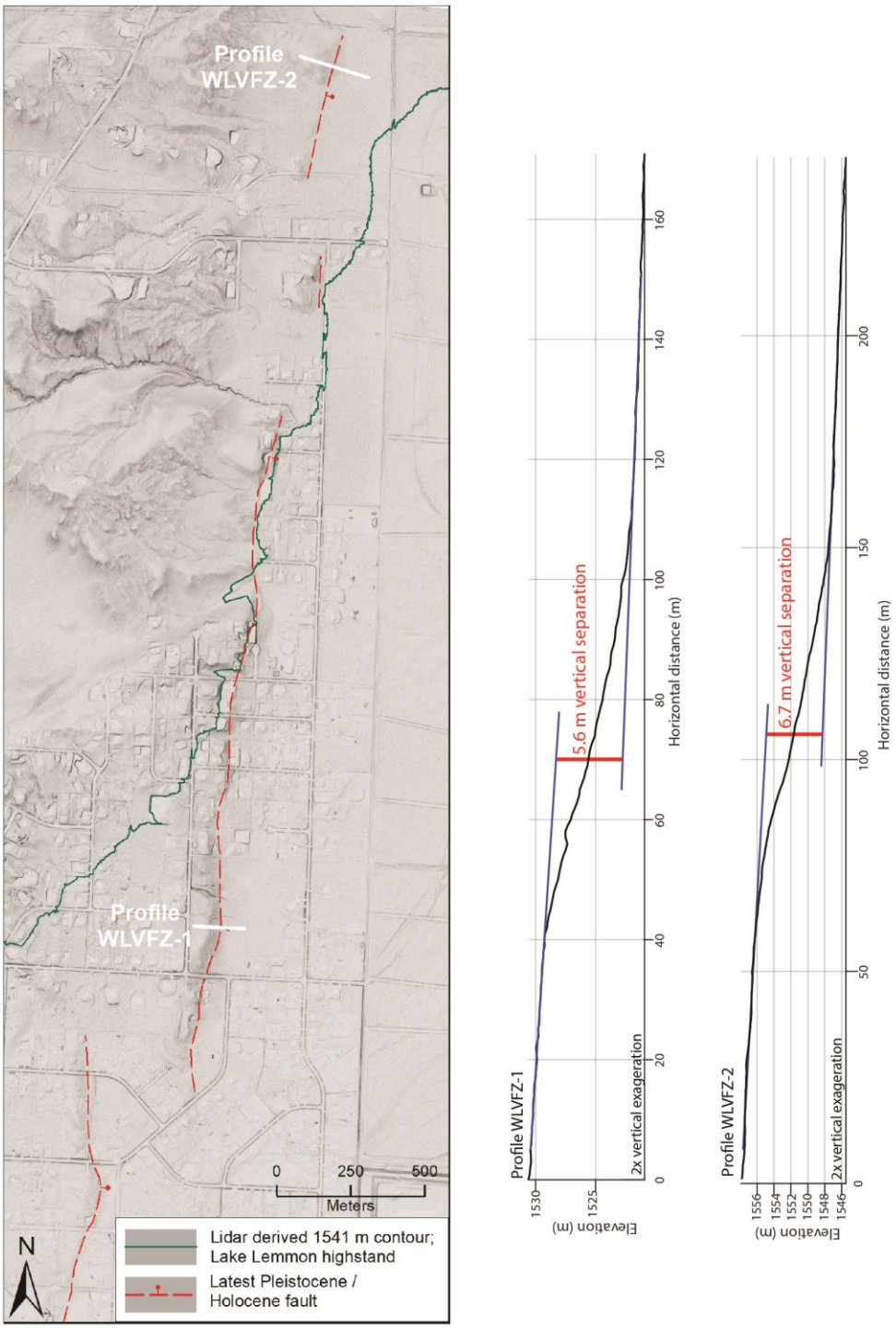

Figure 6 – Lidar slopeshade map of east facing scarps of the WLVFZ (Silver Lake strand) in Lemmon Valley. Figure location shown on Figure 3. Scarps cross the 1541 m Lake Lemmon highstand elevation shown in green. Two profiles across the scarps showing vertical separations of 5.6 and 6.7 m (calculated using the *Scarp Offset* script).

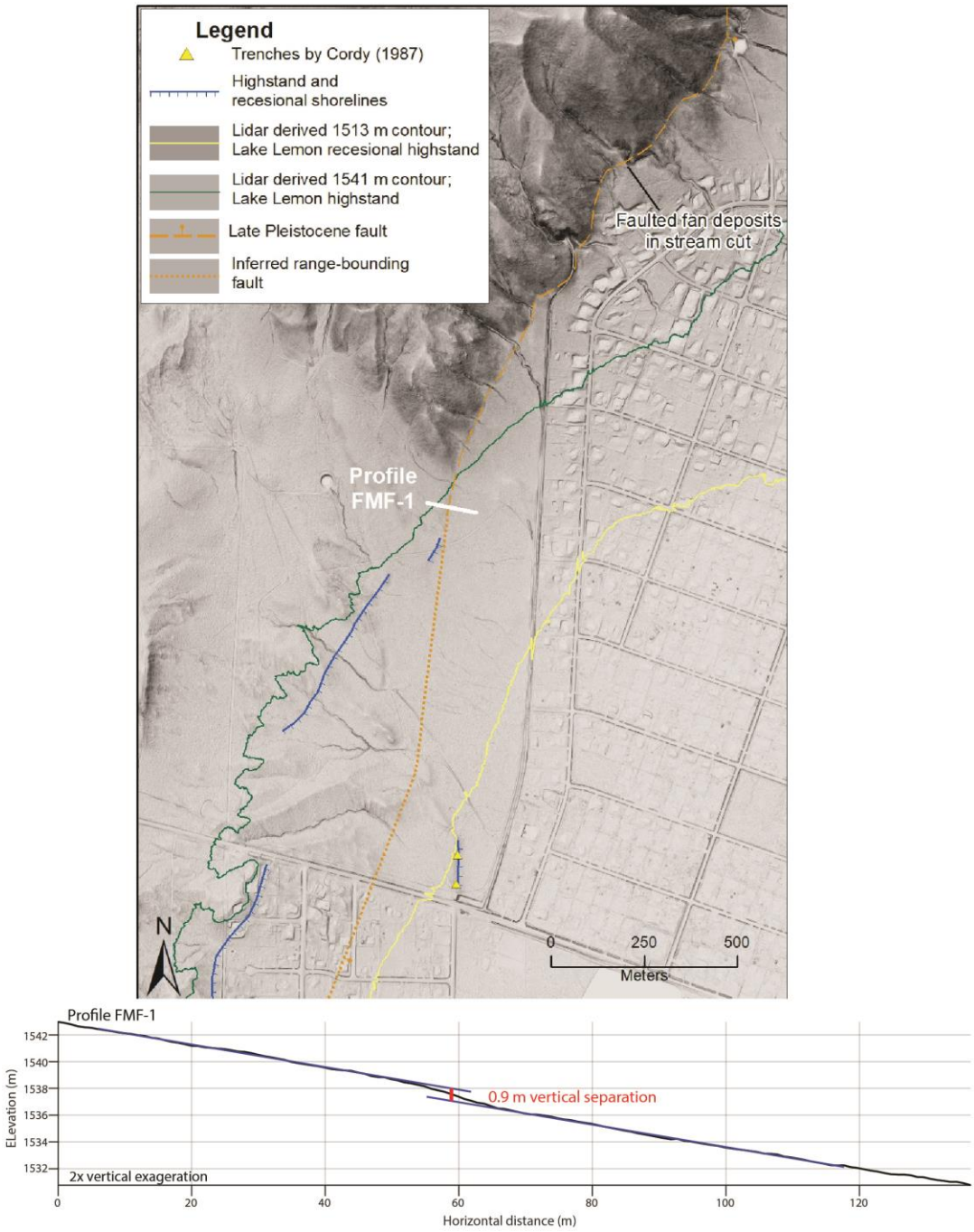

Figure 7 – Lidar slopeshade map of the southern Freds Mountain Fault in Lemmon Valley (location shown on Figure 3). Fan deposits are faulted against bedrock highlands in the north of the map, and a fault scarp continues south into an alluvial-fan surface. The fault scarp ends near the 1541 m Lake Lemmon highstand elevation and associated shoreline remnants. A profile across the fault scarp shows a 0.9 m vertical separation of the alluvial-fan surfaces (calculated using the *Scarp Offset* script). Also shown are the location of the two trenches excavated by Cordy (1987) across what is likely a shoreline from the 1513 m elevation recessional highstand.

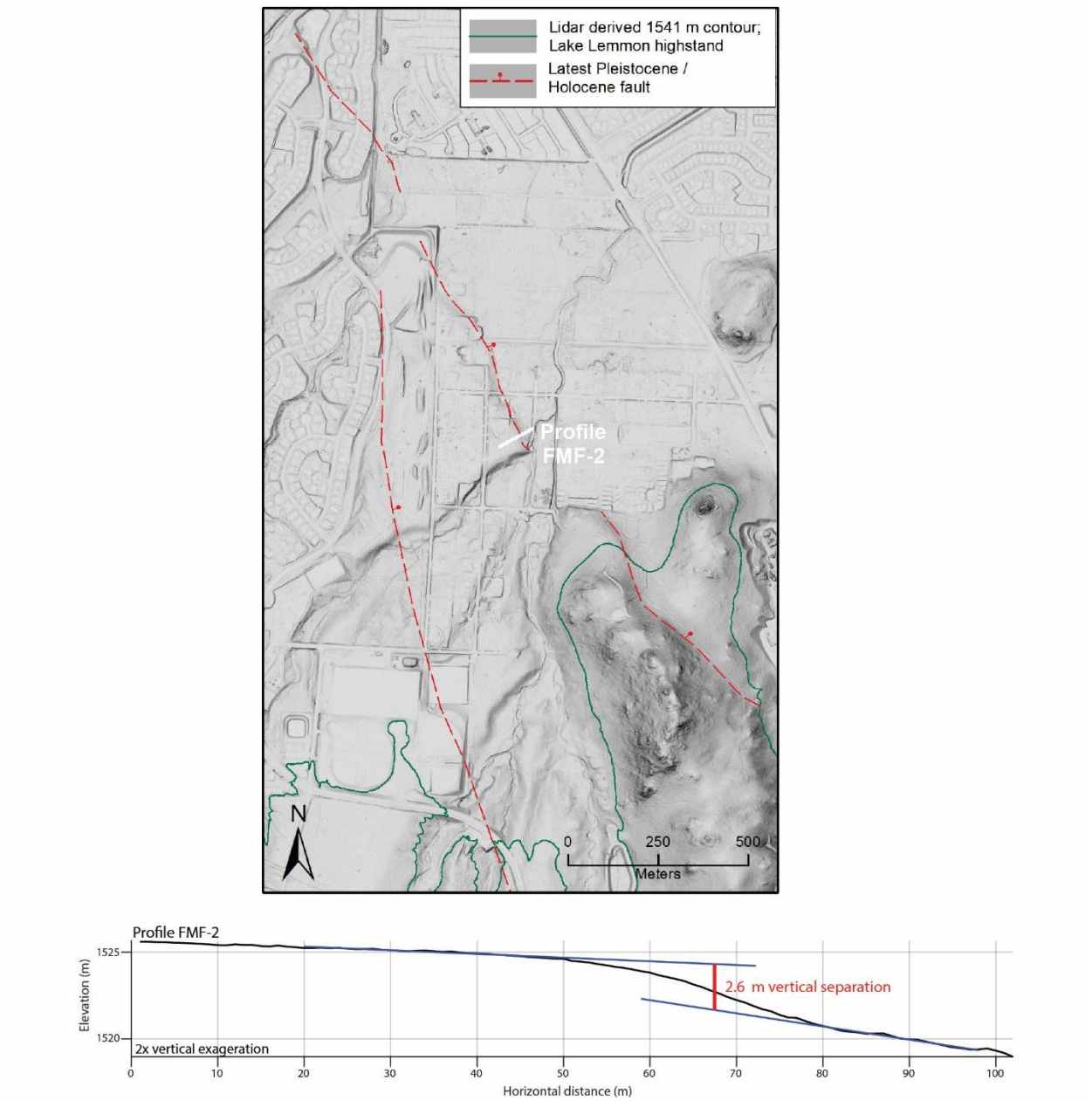

Figure 8 – Lidar slopeshade map of east facing scarps in southern Lemmon Valley (location shown on Figure 3). Scarps cross the 1541 m Lake Lemmon highstand elevation shown in green. A profile across the scarps shows a 2.6 m vertical separation of an alluvial-fan surface (calculated using the *Scarp Offset* script).

Table 1 – Summary of Lemmon Valley fault scarp profile data and estimated vertical slip-rates

Profile	Fault	Latitude	Longitude	Vertical Separation (m)	Approx. age of displaced surface	Vertical Slip-rate (mm/yr)
WLVFZ-1 (Fig. 6)	WLVFZ Silver Lake strand	39°39'59"N	119°54'33"W	5.6	late Pleistocene alluvial-fan 12-120 ka	0.05-0.5
WLVFZ-2 (Fig. 6)	WLVFZ Silver Lake strand	39°41'35"N	119°54'20"W	6.7	late Pleistocene alluvial-fan 12-120 ka	0.06-0.6
WLVFZ-3 (Fig. 4)	WLVFZ Granite Hills strand	39°39'10"N	119°55'45"W	2.3	late Pleistocene alluvial-fan 12-120 ka	0.02-0.2[1]
FMF-1 (Fig.7)	Southern FMF	39°41'6"N	119°50'59"W	0.9	late Pleistocene alluvial-fan 12-120 ka	0.02-0.08
FMF-2 (Fig.8)	Peavine Peak fault zone?	39°37'50"N	119°51'40"W	2.8	middle to late Pleistocene alluvial-fans 12-780 ka	<0.01-0.2

[1]Profile WLVFZ-3 crosses the Granite Hills strand of WLVFZ and only partially captures total displacement and rate

ANTELOPE VALLEY SECTION OF THE FREDS MOUNTAIN FAULT

North of Lemmon Valley the FMF continues as a generally north-striking, east-dipping range bounding normal fault along the west side of Antelope Valley (Figure 2). This section of the fault was profiled by Nitchman and Ramelli (1991), who determined a late Pleistocene aged alluvial-fan surface was displaced 7 m vertically. Koehler (2018) profiled additional scarps in Antelope Valley using lidar data, finding 5 to 9 m displacements in late Pleistocene fans, and calculated slip-rates ranging from 0.03-0.3 mm/yr.

New mapping of the faults and Quaternary geology in Antelope Valley is shown in Figure 9. Surficial deposits in the basin include alluvial-fan deposits: Qfy – Holocene / active alluvial-fans; Qfi – intermediate age fans that are likely latest Pleistocene to earliest Holocene in age, and Qfo - older fans that are likely middle to late Pleistocene in age. The presence of a late Pleistocene lake in Antelope Valley is demonstrated by fine grained lacustrine and beach bar deposits distributed throughout the valley bottom. New mapping of these deposits and shoreline remnants suggests the lake reached a maximum elevation of 1567 m (see shorelines mapped on Figure 9).

In southernmost Antelope Valley the FMF is expressed as a single trace where Qfo fan deposits are faulted against granitic bedrock. To the north the fault splits into two strands. The western strand bounds the faceted Freds Mountain escarpment with Qfo fans faulted against granitic bedrock. This western strand likely continues along the entire length of the range front, however in northern Antelope Valley the western trace is largely concealed by Qfi fan deposits and is locally exposed entirely within bedrock. Only one fault scarp entirely within Qfo deposits was identified (Figure 9).

The eastern trace is concealed in south-central Antelope Valley (Figure 9). It is inferred to bound a uplifted bedrock bench, however no fault scarps in Quaternary deposits were identified. The eastern escarpment of the uplifted bench appears modified from erosion by the late Pleistocene lake within Antelope Valley, and the base of the escarpment is mapped as a shoreline in Figure 9. Fault scarps in Quaternary surfaces along this trace may have been obscured by burial or erosion related to lacustrine processes.

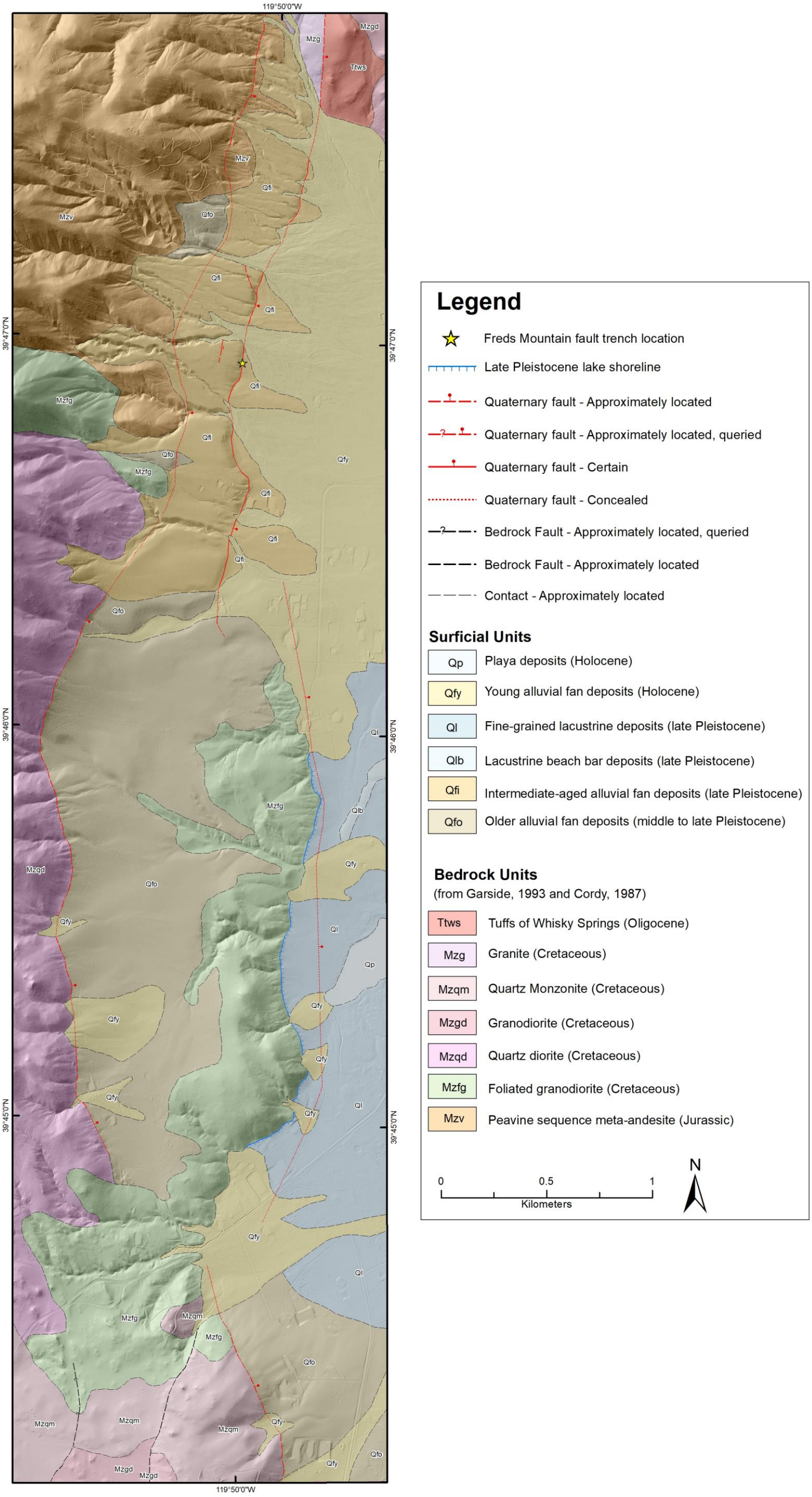

Figure 9 –Freds Mountain fault in Antelope Valley. New mapping of the Quaternary fault trace and surficial geology. Bedrock geology modified from Garside (1993) and Cordy (1987)

To the north the eastern trace has a distinctly different expression with fault scarps up to 11 high in Qfi fan surfaces. These are the scarps profiled in previous studies yielding vertical displacements of 5 to 9 m (Nitchman and Ramelli, 1991; Koehler, 2018). A paleoseismic trench was excavated across one of these scarps as part of this study. The eastern trace continues north of the basin into a bedrock knob where it faults Tertiary tuffs against Mesozoic granodiorite (Garside, 1993; Figure 9).

North of Antelope Valley the USGS Quaternary fault database shows the FMF as continuing through a low divide and into Bedell Flat as a piedmont slope fault that bounds uplifted Tertiary sediments (Figure 2). The northernmost section of the FMF is truncated against, or merges with the northwest-striking dextral Warm Springs Valley fault. While the Bedell Flat section was not examined in detail for this study, scarps in alluvial-fan sediments are apparent in lidar suggesting the section may have a paleoseismic history similar to the Antelope Valley section.

Freds Mountain Fault Trench

In June of 2018 a paleoseismic trench was excavated across a 9 m tall scarp in a Qfi fan surface along the Freds Mountain fault (Figures 9 and 10). The trench site was selected due to the apparent isolation of the hanging wall from modification and deposition by active Qfy fan deposits distributed at the mouth of adjacent gullies. The trench was 65 m long, excavated to an average depth of approximately 4 m, and benched for wall stability. The trench walls were cleaned and a grid of nails was established at 2 m horizontal, 1 m vertical intervals. Key stratigraphic units and faults were flagged and the trench was photographed for construction of a photomosaic using Agisoft software. Scale bars with control points spaced 0.5 m apart were used for spatial rectification of the Agisoft model. The trench was logged in the field on color prints of the photomosaic and later digitized. The uninterpreted photomosaic and interpreted trench logs of the north and south wall are shown in Figures 11 and 12. Bulk radiocarbon samples were collected from key stratigraphic horizons and sent to PaleoResearch Institute for sieving, organic material identification and possible AMS dating if suitable material is recovered. Samples for Optically Stimulated Luminescence (OSL) dating were also collected in aluminum and PVC tubes and samples are being processed at the USGS luminescence laboratory in Denver, CO.

Stratigraphic and Structural Relations

The footwall stratigraphy exposed in the trench is composed of fanglomorate deposits of well sorted sandy gravel and gravelly sand with cobbles and boulders (Units AF1-AF8 on the south wall and AFa-AFe on the north wall). The fan units were easily distinguished in the field using abrupt changes in gravel or sand content. The alluvial-fan contacts have gentle east dips between 6° and 7°. The footwall stratigraphy could not be correlated between the north and south walls due to the lateral variability in the alluvial-fan deposits. A young surficial colluvium (Unit C1) overlies the footwall fan stratigraphy and continues across the scarp, fault zone and partially buries the hanging wall stratigraphy. West of the scarp a soil with an approximately 70 cm thick Bt overlain by a 10 cm thick Bw horizon is preserved in the youngest fan deposits (soil profile shown on Figure 11 south wall).

The hanging wall stratigraphy is composed of a package of scarp derived colluvium (Units SC1-SC4) which overlie an alluvial-fan deposit (AF0). The basal alluvial-fan deposit (AF0) is bedded and moderately sorted distinguishing it from the massive, unsorted scarp colluvium above. Only 50 cm of Unit AF0 is exposed at the base of the trench but it may correlate with the youngest fan deposit in the footwall (AF1). A package of sandy alluvium with gravel interbeds (A1a-A1c) is inset against and interfingers with the colluvial-wedge deposits. These alluvial deposits are eroded into the distal end of the colluvial-wedge package suggesting fluvial transport at the base of the scarp, likely in the Holocene. Scarp colluvium SC4, SC3 and SC2 are poorly sorted, cobble-rich packages that were distinguished based on basal stone lines, composition

changes and variations in matrix color. The composition and lithology of angular to sub-angular boulders within these SC deposits roughly match the alluvial-fan material exposed in the scarp free face. The youngest colluvial wedge, SC1, is not as clearly defined and therefore queried on the logs. An attempt to distinguish SC1 was necessitated by the faulting that displaces SC2, requiring an event after its deposition. In the south wall SC1 is logged around a collection of boulders within the otherwise sand rich alluvium of Unit A1a. In the north wall SC1 is logged as a fissure fill associated with the youngest faulting event. Each of the 4 scarp colluvial packages are interpreted to represent a surface-rupturing earthquake event labeled EQ1 (youngest) through EQ4 (oldest) in Table 2.

Three distinct fault zones were identified in the south wall, f1, f2 and f3 from east to west, and only one broad fault zone in the north wall, suggesting the three zones merge northward. The faults dip 63°-69° east and strike roughly parallel to the mapped fault trace at 5° to 10°. Faults are defined by shear planes, truncated stratigraphy and steeply rotated clasts. No kinematic indicators could be identified in the fault zones but the displacement sense is considered likely to be purely dip-slip.

Two possible slip-per-event measurements can be made using the available stratigraphy (Table 2). F1 displaces SC2 1.4 m vertically providing a reasonable estimate of displacement during EQ1. F3 displaces alluvial-fan stratigraphy an average of 1.5 m vertically and is capped by the probable footwall equivalent of SC2. If the 1.5 m of measured vertical displacement on f3 is from a single event it could be associated with EQ3 or EQ4. The thickness of the scarp colluviums provide lower limits for vertical displacement in each earthquake. Scarp colluvium thickness varies from 0.9 m for EQs 1 and 2, 0.7 m for EQ3, and 1.3 m for EQ 4 (Table 2).

An estimate of the total vertical displacement across the fault zone at the FMF trench site cannot be well constrained using the typical scarp topographic profile / surface correlation method. This is due to the surprising thickness of sand-rich alluvium accumulated at the base of the scarp (Units A1a-A1c), the top of which does not correlate with the alluvial-fan surface in the footwall. An alternative measure of total displacement can be made using the assumption that the top of the AF0 unit, which underlies the scarp colluvium package, is correlative with the top of AF1 in the uplifted footwall (Figure 13). An estimate of the displaced (pre-scarp) surface gradient is made using the average 6.5° east dips of the alluvial-fan stratigraphy which would mirror the gradient of the ground surface at the time of fan deposition. The 6.5° dipping surface line is fit to the top of unit AF1 west of the eroding scarp face and to the top of AF0 in the hanging wall. This method yields a vertical separation measurement of 9.8 m in the south wall and 9.3 m in the north wall, averaging 9.6 m total vertical displacement.

OSL and bulk radiocarbon sample locations are shown on Figure 11 and results are pending. The geochronology data is anticipated to place constraints on a recurrence interval and slip-rate for the Antelope Valley section of the Freds Mountain fault.

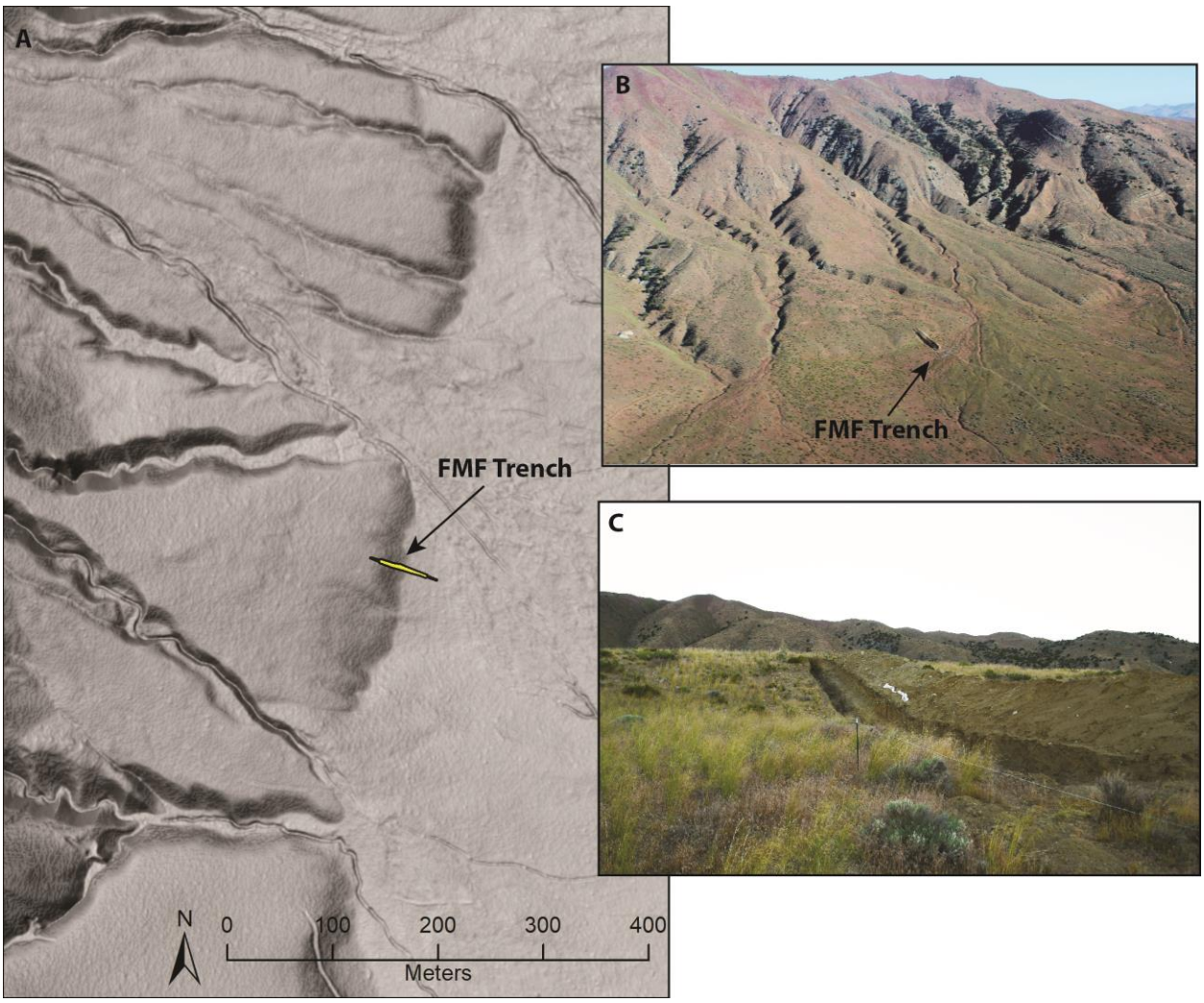

Figure 10 – A) Lidar slopeshade map of the FMF trench site location; B) Aerial photograph by John Bell of the FMF trench; C) photo of the FMF trench

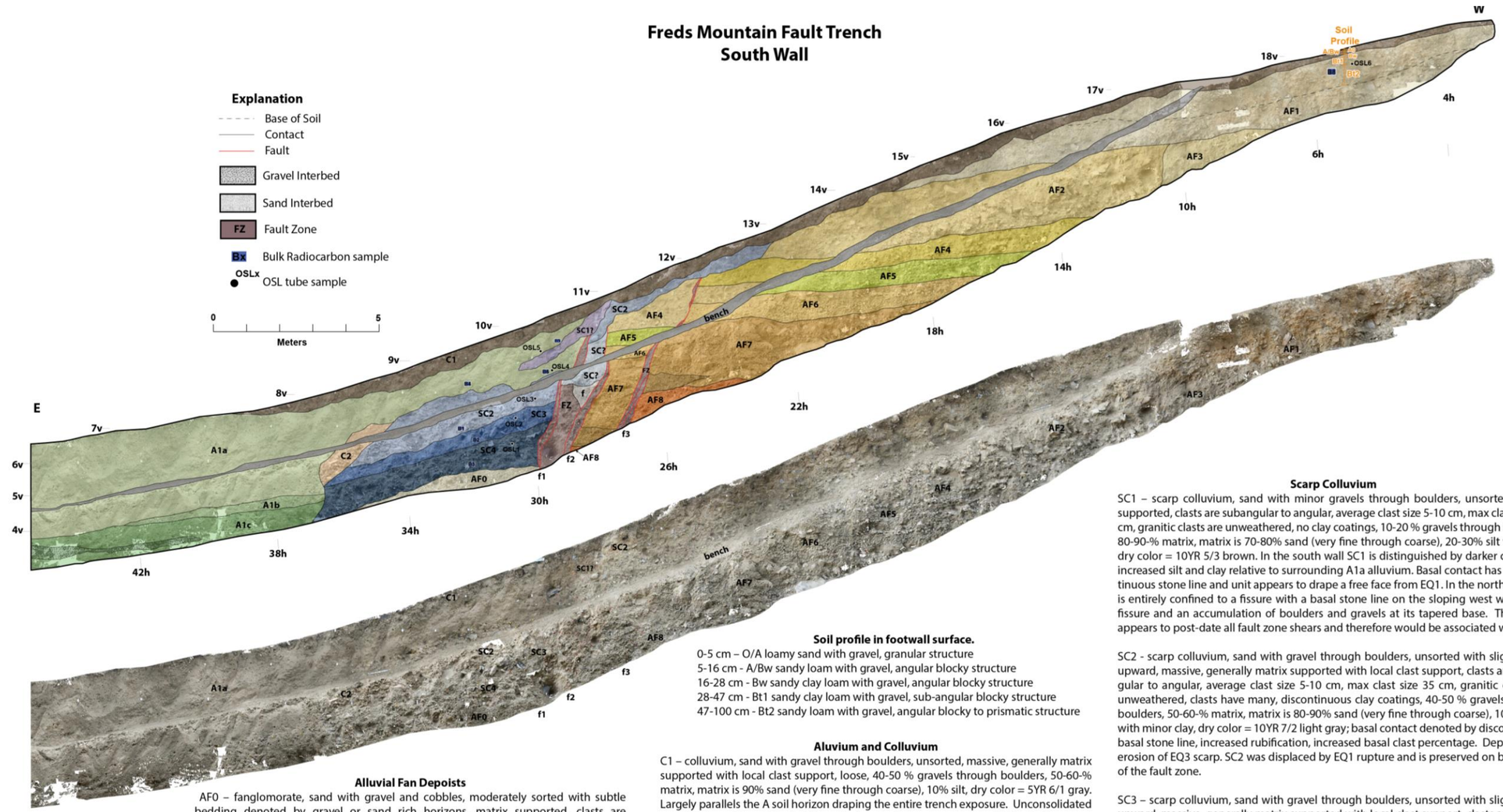

Alluvial Fan Deposits

AF0 – fanglomorate, sand with gravel and cobbles, moderately sorted with subtle bedding denoted by gravel or sand rich horizons, matrix supported, clasts are subrounded, average 5-10 cm, max 15 cm long axis, granitic clasts are partially weathered / decomposed, 30-40% gravels through cobbles, 60-70% matrix, matrix is fine to coarse sand with minor silt, dry color = 2.5 Y 7/2 light gray. Alluvial fan deposit, possibly correlative with AF1 in footwall.

AF (1-8 in south wall and a-e in north wall) - fanglomorate, interbedded sandy gravel and gravelly sand with cobbles and boulders, well sorted with bedding defined by gravel or sand rich horizons, matrix and clast supported, clasts are subrounded to subangular, average 10-20 cm, max 90 cm long axis, granitic clasts are variably weathered with some boulders moderately decomposed, variable clay coatings with clasts in some beds fully coated, 30-80 % gravels through boulders, 20-70% matrix, matrix is fine to coarse sand with minor silt, dry color = 2.5Y 7/1 light gray to 2.5Y 6/2 light brownish gray. Alluvial fan deposits sourced from Freds Mountain, deposited by intermittent streams and debris flows into Antelope Valley.

Soil profile in footwall surface.

0-5 cm – O/A loamy sand with gravel, granular structure
5-16 cm - A/Bw sandy loam with gravel, angular blocky structure
16-28 cm - Bw sandy clay loam with gravel, angular blocky structure
28-47 cm - Bt1 sandy clay loam with gravel, sub-angular blocky structure
47-100 cm - Bt2 sandy loam with gravel, angular blocky to prismatic structure

Aluvium and Colluvium

C1 – colluvium, sand with gravel through boulders, unsorted, massive, generally matrix supported with local clast support, loose, 40-50 % gravels through boulders, 50-60-% matrix, matrix is 90% sand (very fine through coarse), 10% silt, dry color = 5YR 6/1 gray. Largely parallels the A soil horizon draping the entire trench exposure. Unconsolidated surficial deposit associated with gradual downslope movement and bioturbation.

C2 – colluvium, unsorted gravel and boulder rich deposit resting uncomfortably on the distal end of SC2 and SC3. Likely deposited on an eroded channel margin associated with deposition of Unit A1.

A1a, A1b and A1c – alluvium, sand with minor gravels and gravel rich interbeds, well sorted, generally massive with discontinuous 5-20 cm thick beds denoted by increase gravel or coarse sand, clasts are subrounded, clast size 3-10 cm, 90% matrix (fine to medium sand with less than 10% silt), 10% gravel, dry color = 10YR 6/3 pale brown, basal contact over SC2 denoted by change from coarse gravels through boulders in SC2 to primarily sand in A1a. Unit has a channel form base that is eroded into and buttressed against the distal end of the SC4-SC2 scarp colluvium package. Cut and fill deposited associated with stream flow at the base of the FMF scarp.

Scarp Colluvium

SC1 – scarp colluvium, sand with minor gravels through boulders, unsorted, matrix supported, clasts are subangular to angular, average clast size 5-10 cm, max clast size 40 cm, granitic clasts are unweathered, no clay coatings, 10-20 % gravels through boulders, 80-90-% matrix, matrix is 70-80% sand (very fine through coarse), 20-30% silt with clay, dry color = 10YR 5/3 brown. In the south wall SC1 is distinguished by darker color, and increased silt and clay relative to surrounding A1a alluvium. Basal contact has a discontinuous stone line and unit appears to drape a free face from EQ1. In the north wall SC1 is entirely confined to a fissure with a basal stone line on the sloping west wall of the fissure and an accumulation of boulders and gravels at its tapered base. The fissure appears to post-date all fault zone shears and therefore would be associated with EQ1.

SC2 - scarp colluvium, sand with gravel through boulders, unsorted with slight fining upward, massive, generally matrix supported with local clast support, clasts are subangular to angular, average clast size 5-10 cm, max clast size 35 cm, granitic clasts are unweathered, clasts have many, discontinuous clay coatings, 40-50 % gravels through boulders, 50-60-% matrix, matrix is 80-90% sand (very fine through coarse), 10-20% silt with minor clay, dry color = 10YR 7/2 light gray; basal contact denoted by discontinuous basal stone line, increased rubification, increased basal clast percentage. Deposited by erosion of EQ3 scarp. SC2 was displaced by EQ1 rupture and is preserved on both sides of the fault zone.

SC3 – scarp colluvium, sand with gravel through boulders, unsorted with slight fining upward, massive, generally matrix supported with local clast support, clasts are subangular to angular average clast size 15-20 cm, max clast size 65 cm, granitic clasts are slightly weathered / decomposed, clasts have abundant, discontinuous clay coatings 50-60 % gravels through boulders,40-50-% matrix, matrix is 70-80% sand (very fine through coarse), 20-30% silt with minor clay, dry color = 2.5 Y 7/2 light gray; basal contact denoted by boulder rich basal stone line, slight color change, coarsening of matrix material. Deposited by erosion of EQ3 scarp.

SC4 – scarp colluvium, silty sand with gravel through boulders, unsorted, massive, matrix supported, clasts are subangular to angular, average 5-10 cm max 30 cm long axis, granitic clasts are partially weathered / decomposed, clasts commonly have continuous clay coatings , 40-50 % gravels through boulders, 50-60 % matrix, matrix is slightly more fine sand than silt, dry color = 2.5 Y 7/2 light gray. Basal contact denoted by lack of sorting relative to underlying bedded fanglomorate, weak basal stone line and increased coarse material. Deposited by erosion of EQ4 scarp.

Figure 11 - Freds Mountain fault south wall trench log and unit descriptions

Freds Mountain Fault Trench
North Wall

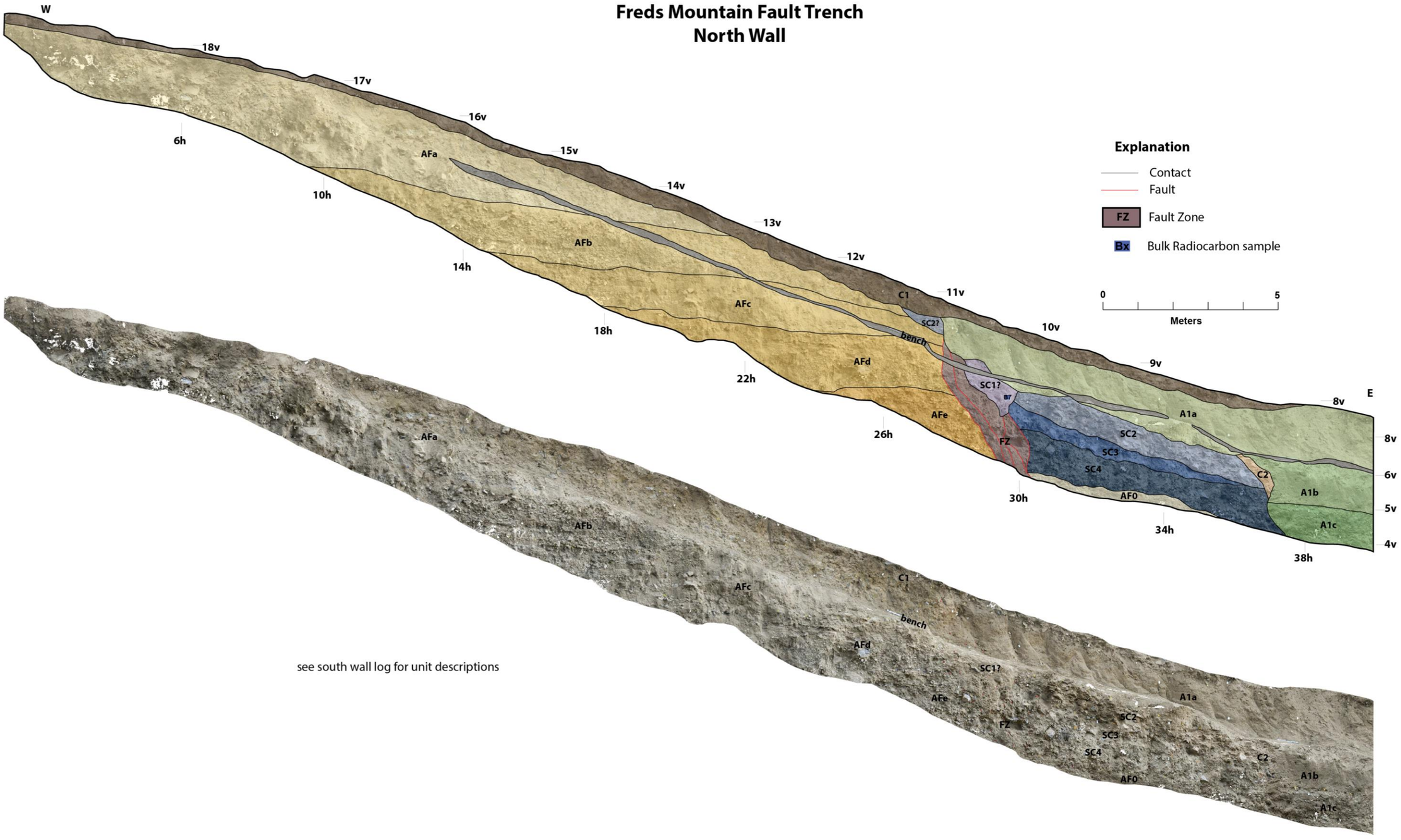

see south wall log for unit descriptions

Figure 12 - Freds Mountain fault north wall trench log

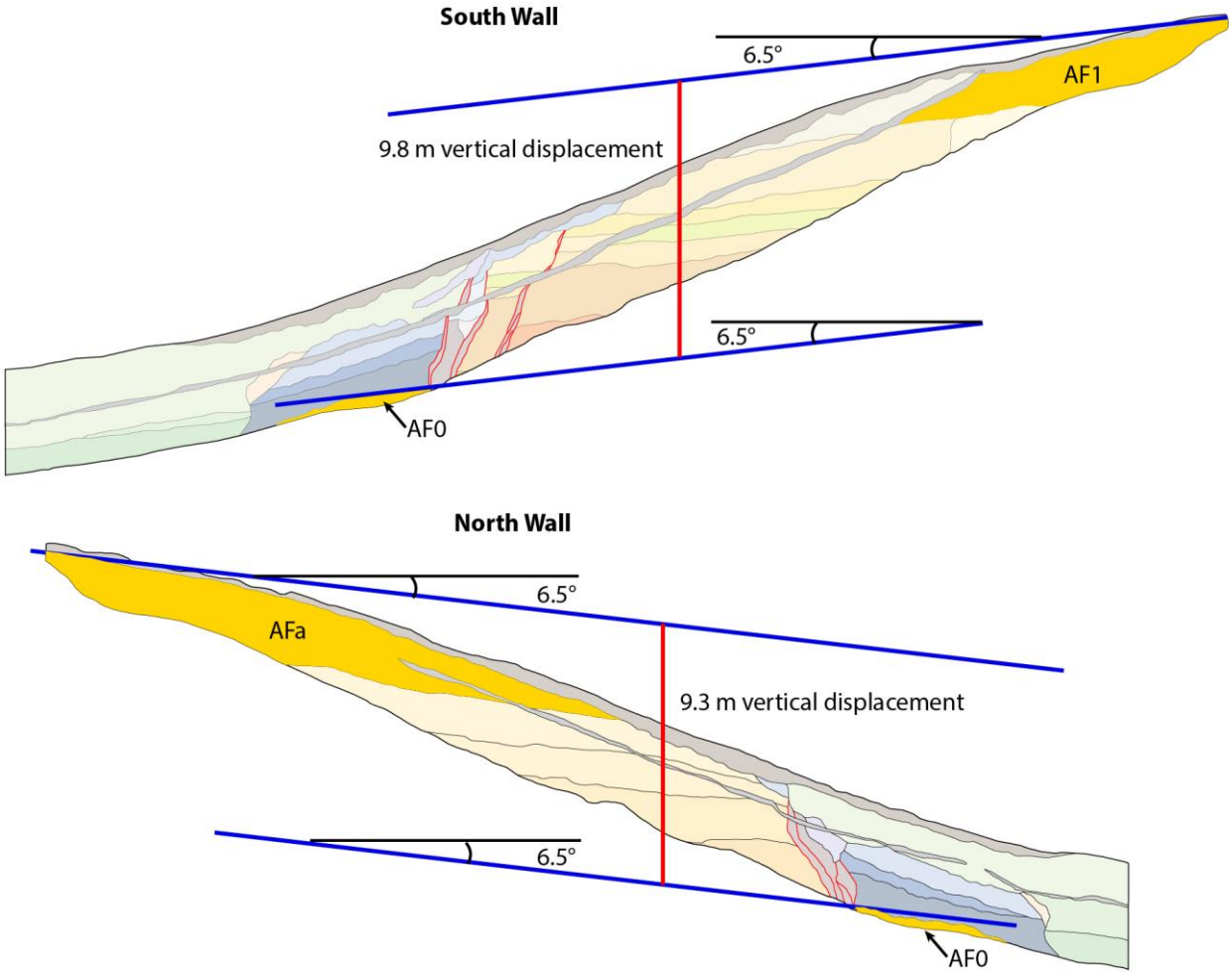

Figure 13 – Vertical separation measurements from the FMF trench. Assumes top of youngest exposed alluvial-fan deposits in hanging wall and footwall are correlative. 6.5° pre-displacement slope calculated using average dip of alluvial-fan contacts which would closely resemble surface at time of deposition. Average vertical displacement from both walls = 9.6 m.

Table 2 – Summary of earthquakes interpreted from the FMF trench

Earthquake	Scarp Colluvium (Figure 11)	SC Thickness (m)	Vertical Displacement Estimate (m)	Age
EQ1 (most recent event)	SC1	south wall: 0.9	1.4	pending
EQ2 (penultimate event)	SC2	south wall: na north wall: 0.9[1]	na	pending
EQ3	SC3	south wall: 0.7 north wall: 0.7	1.5?[2]	pending
EQ4	SC4	south wall: 1.3 north wall: 1.3	1.5?[2]	pending

[1]Minimum thickness due to erosion on the top of scarp colluvium associated with deposition of Unit A1a

[2] measured displacement of 1.5m on fault f3 could be attributed to either EQ3 or EQ4

DISCUSSION AND CONCLUSIONS

Fault mapping in Lemmon Valley in conjunction with a better understanding of the Lake Lemmon highstand elevation provides several important observations that can be incorporated into future fault databases and source parameters. The WLVFZ was not included in the 2014 update to the National Seismic Hazard Map. The new mapping suggests that the fault is a semi-continuous, capable seismogenic structure. Slip-rate estimates for the Silver Lake strand of the WLVFZ, summarized in Table 1, range from 0.05 to 0.6 mm/yr with no firm age control on displaced deposits. The preservation of the Silver Lake strand scarps within the extent of the Lake Lemmon highstand suggest at least some of the displacement may post-date the latest Pleistocene Lake Lemmon highstand, thus weighting the higher slip-rate estimates. The observation that other fault scarps in the basin, including the southern FMF and Granite Hills strand of the WLVFZ (Figure 3), appear to end at the Lake Lemmon highstand elevation provides additional evidence that the lake may have eroded or buried low relief topographic features including pre-existing fault scarps.

The FMF has significant along-strike variability in slip-rate and paleoseismic history and it is recommended that the FMF be treated as a segmented structure in future source models and fault maps. A Lemmon Valley segment (excluding the scarps south of Swan Lake, shown on Figure 8) has a small scarp preserved in a late Pleistocene alluvial-fan surface and no evidence for scarps within the extent of the Lake Lemmon highstand or in Holocene deposits (Figure 7). This suggests that the fault segment has a long recurrence interval with no record of Holocene rupture. In contrast an Antelope Valley segment (Figures 2 and 9) is significantly more active, as evidenced by the large scarps in late Pleistocene fan deposits and the FMF trench results. A Bedell Flat segment of the FMF may have a similar level of activity as the Antelope Valley segment but requires further study (Figure 2). The southernmost fault scarps in central Lemmon Valley, shown on Figure 8, have northwest-trending, east-facing scarps in middle to late Pleistocene fan deposits. These scarps are included with the FMF in the USGS Quaternary fault database, but the orientation and size of these scarps is similar to several nearby traces of the Peavine Peak fault zone and it is recommended that they be considered part of that fault system in future maps.

The four scarp colluvial packages in the FMF trench are interpreted to record four-surface rupturing earthquakes on the fault. Total vertical displacement on the fault has been measured at an average of 9.6 m. Two vertical slip-per-event measurements on displaced stratigraphy were measured at 1.4 and 1.5 m. If these event displacements are characteristic of earthquakes on the FMF then 6 to 7 earthquakes are required to produce the measured total vertical displacement, which suggest the earthquake history recorded in the trench may be incomplete. Alternatively, vertical displacements may be larger in some events. The age of these ruptures and an earthquake recurrence interval will be evaluated when radiocarbon and OSL samples are finalized.

REFERENCES

Adams, K.D., Wesnousky, S.G., 1999. The Lake Lahontan Highstand: age, surficial characteristics, soil development, and regional shoreline correlation. Geomorphology 30, 357–392.

Adams, K.D., Goebel, T., Graf, K., Smith, G., Camp, A.J., Briggs, R., Rhode, D.E., 2008. Late Pleistocene and early Holocene lake-level fluctuations in the Lahontan basin, Nevada. Implications for the distribution of archaeological sites. Geoarchaeology 23 (5), 608–643.

Bormann, J., 2013. New Insights Into Strain Accumulation and Release in the Central and Northern Walker Lane, Pacific-North American Plate Boundary, California and Nevada, USA. Ph.D. Dissertation. University of Nevada, Reno.

Cordy, G.E., 1985, Geologic map, Reno NE quadrangle: Nevada Bureau of Mines and Geology Map 4Cg, scale 1:24,000.

Cordy, G.E., 1987, Geology and earthquake hazards Reno NE quadrangle: Nevada Bureau of Mines and Geology OpenFile Report 875, 78 p.

dePolo, C. M., 2006, Determination of fault slip rates, paleoearthquake history, and segmentation of the Warm Springs Valley fault system, NEHRP Technical Report, 04HQGR0082, 35 pp.

dePolo, C. M., and Ramelli, A. R. , 2004, Paleoseismic studies along the Warm Springs Valley fault system, NEHRP Technical Report, 01HQGR0019, 41 pp.

Faulds, J. E., Henry, C. D., and Hinz, N. H., 2005, Kinematics of the northern Walker Lane: An incipient transform fault along the Pacific–North American plate boundary, Geology 33, 505–508.

Field, E.H., Biasi, G.P., Bird, P., Dawson, T.E., Felzer, K.R., Jackson, D.D., Johnson, K.M., Jordan, T.H., Madden, C., Michael, A.J., Milner, K.R., Page, M.T., Parsons, T., Powers, P.M., Shaw, B.E., Thatcher, W.R., Weldon II, R.J., Zeng, Y., 2013. Uniform California earthquake rupture forecast, version 3 (UCERF3)—the time-independent model. U.S. Geological Survey Open-File Report 2013–1165, 97 p., California Geological Survey Special Report 228, and Southern California Earthquake Center Publication 1792 http://pubs.usgs.gov/of/2013/1165/.

Garside, L.J., 1993, Geologic map of the Bedell Flat quadrangle, Nevada, Nevada Bureau of Mines and Field Studies Map 3, scale 1:24,000.

Garside, L.J., Nials, F.L., and Ramelli, A.R., 2010, Preliminary geologic map of the Griffith Canyon quadrangle, Washoe County, Nevada, Open-File Report 2010-02, scale 1:24,000.

Gold, R.D., dePolo, C. M., Briggs, R. W., Crone, A. J., and Gosse, J., 2013, Late Quaternary slip-rate variations along the Warm Springs Valley fault system, northern Walker Lane, California-Nevada border: Bulletin of the Seismological Society of America. v. 103, no 1., p. 542-558.

Gold, R.D., Briggs, R.W., Crone, A.J., DuRoss, C.D., 2017. Refining fault slip rates using multiple displaced terrace risers–an example from the Honey Lake fault, NE California, USA. Earth Planet. Sci. Lett. 477, 134–146.

Hammond, W. C., Blewitt, G. and Kreemer, C., 2011, Block Modeling of crustal deformation of the Northern Walker Lane and Basin and Range from GPS velocities, J. Geophys. Res. B Solid Earth Planets 116, 1–28.

Hammond, W. C., and Thatcher, W., 2007, Crustal deformation across the Sierra Nevada, northern Walker Lane, Basin and Range transition, western United States measured with GPS 2000–2004, J. Geophys. Res. B Solid Earth Planets 112, 1–26.

Hubbs, C. L., and Miller, R. R., 1948, The Great Basin, with emphasis on glacial and post-glacial times; Part 11, The zoological evidence: Utah Univ. Bulletin vol. 38, no. 20, p. 18-166.

Koehler, R. D., 2018, Active faulting in the North Valleys region of Reno, Nevada: A distributed zone within the northern Walker Lane. Geomorphology.

Koehler, R.D., and Anderson, J.G., in press, 2018 Working group on Nevada seismic hazards—summary and recommendations of the workshop: Nevada Bureau of Mines and Geology Open-File Report.

Nitchman, S.P., 1991, Petersen Mountain fault: Nevada Bureau of Mines and Geology Preliminary Fault Evaluation Report, 3 p., scale 1:62,500.

Nitchman, S.P., and Ramelli, A.R., 1991, Freds Mountain fault: Nevada Bureau of Mines and Geology Evaluation Report, 7 p., 2 scarp profiles, scale 1:62,500.

Petersen, M.D., Moschetti, M.P., Powers, P.M., Mueller, C.S., Haller, K.M., Frankel, A.D., Zeng, Yuehua, Rezaeian, Sanaz, Harmsen, S.C., Boyd, O.S., Field, Ned, Chen, Rui, Rukstales, K.S., Luco, Nico, Wheeler, R.L., Williams, R.A., and Olsen, A.H., 2014, Documentation for the 2014 update of the United States national seismic hazard maps: U.S. Geological Survey Open-File Report 2014–1091, 243 p., http://dx.doi.org/10.3133/ofr20141091.

Puseman, K., 2010, Macrofloral analysis of alluvium from Jacks Valley trench to recover radiocarbon datable material, and microcharcoal extraction and AMS radiocarbon dating of alluvium from the Peavine trench, Nevada: PaleoResearch Institute Technical Report 10-15.

Ramelli, A.R., Bell, J.W., dePolo, C.M., and Yount, J.C., 1999, Large-magnitude, late Holocene earthquakes on the Genoa fault, west-central Nevada and eastern California: Bulletin of the Seismological Society of America, v. 89, p. 1458-1472.

Ramelli, A. R., dePolo, C. M., and Bell, J.W., 2003, Paleoseismic studies of the Peavine Peak fault, NEHRP Technical Report, 01HQGR0167, 15 pp.

Ramelli, A. R., Bell, J.W., and dePolo, C. M., 2005, Peavine Peak fault: Another Piece of the Walker Lane Puzzle, in Lund, W.R., editor, Western States Seismic Policy Council Proceedings Volume of the Basin and Range Province Seismic-Hazards Summit II: Utah Geological Survey Miscellaneous Publication 05-2.

Ramelli, A. R., Henry, C. D., and Walker, J. P., 2012, Preliminary Revised Geologic Maps of the Reno Urban Area, Nevada: Nevada Bureau of Mines and Geology, Open-file report 11-7, scale 1:24,000, 3 plates.

Ramelli, A. R., and Bell, J.W., 2014, Spatial and Temporal Patterns of Fault Slip Rates on the Genoa Fault, NEHRP Technical Report, G09AP00020, 21 pp.

Reheis, M.C., Adams, K.D., Oviatt, C.G., Bacon, S.N, 2014, Pluvial lakes in the Great Basin of the western United States—a view from the outcrop. Quaternary Science Reviews. 97. 33–57.

Rood, D. H., Harvey, J.E., Ramelli, A.R., Burbank, D.W., Bookhagen, B., 2011, Temporal fault slip rate and rupture patterns on the Genoa fault, central Eastern Sierra Nevada, integrating ground-based LiDAR, 10Be surface exposure dating, and paleoseismology: American Geophysical Union, Fall Meeting 2011, abstract #T43I-07.

Szecsody, G.C., 1983. Earthquake hazards map, Reno NW quadrangle. Nevada Bureau of Mines and Geology Earthquake Hazards Map 4Di, Scale 1:24,000.

Soeller, S.A., and Nielson, R.L., 1980, Geologic map, Reno NW quadrangle: Nevada Bureau of Mines and Geology Map 4Dg, scale 1:24,000.

Turner, R., Koehler, R., Briggs, R. W., and S. G. Wesnousky, 2008, Paleoseismic and slip-rate observations along the Honey Lake fault zone, northeastern California, Bulletin of the Seismological Society of America, 98, 4, 1730-1736.

U.S. Geological Survey, 2006, Quaternary fault and fold database for the United States, accessed 5/16/2015, from USGS web site: http//earthquakes.usgs.gov/regional/qfaults/.

Wesnousky, S. G., 2005, Active faulting in the Walker Lane, Tectonics, 24, TC3009.

Wills, C. J., and Borchardt, G., 1993, Holocene slip rate and earthquake recurrence on the Honey Lake fault zone, northeastern California, Geology 21, 853–856.

Woodcock, N.H. and Fisher, M, 1986, Strike-slip duplexes, Journal of Structural Geology, Vol. 8, No. 7, pp. 725 to 735.